Bluff Body Noise and Flow Control with Atmospheric Plasma Actuators

Xun Huang* Xin Zhang† and Steve Gabriel‡

University of Southampton, Southampton, SO17 1BJ, United Kingdom

Plasma actuators operating in atmospheric air were employed to modify aerodynamic flow over a bluff body. The model consisted of a cylinder and a strut that was installed on the trailing half side of the cylinder. The objective was to reduce the broadband noise that is mainly generated by the impingement of the cylinder wake on the strut. The plasma actuators were configured to produce dielectric barrier discharges, through which the flow separation from the cylinder was enhanced. As a result the wake-strut interaction was reduced, leading to the attenuation of broadband noise. The noise and flow control performance with the plasma actuators were studied in an anechoic chamber facility as well as a wind tunnel facility by examining sound pressure and mean flow field respectively. With the current plasma actuators, it was found that there was 1 dB reduction in overall sound pressure level at a free stream speed of 30 m/s, and the wake speed impinging on the strut was reduced. A possible solution to improve the broadband noise attenuation performance is discussed at the end of this paper.

I. Introduction

THE high level of nuisance noise generated by the take-off and landing of aircraft has a significant impact on the communities near airports.[1] With a reduction target of perceived noise level of 50% by 2020,[2] various control techniques have been tested to attenuate aerodynamically generated noise. Plasma actuators, operating in atmospheric pressure air condition, hold the potential to reduce flow-induced noise through modifying aerodynamic flow field. Some recent work[3–6] have demonstrated the potential of using the dielectric barrier discharge (DBD) plasma actuators[7] to attenuate the tonal noise of a cavity that is similar to a landing gear bay.

Dielectric barrier discharge plasma actuators are able to generate weakly ionized atmospheric plasma, which is coupled to an electric field thus inducing body force that affects the flow field local to the plasma actuators.[8–12] In addition to a high alternating current (AC) power supply, a plasma actuator system consists of a pair of copper electrodes, between which a dielectric material is placed to prevent electric arching. The voltage applied to the electrodes operates at O(kHz) frequency to sustain the glow discharge. The simplicity and absence of mechanical moving parts, *e.g.* pumps, make the plasma actuator a promising option for aerospace applications. In this work the DBD plasma actuators were applied to a bluff body, which is an idealised model of the main leg part of a landing gear. The same type of plasma actuators were applied on a single cylinder at Reynolds number from 1×10^4 to 4×10^4 previously[10,13] to control wake flow and suppress vortex shedding.

In the previous cavity experiments, the plasma actuators attenuated flow-induced tonal noise through either manipulating shear layer[3–5] or generating disturbances at off-resonant frequency.[6] The amplification of the flow system at the normal resonant frequency is consequently suppressed. Rather than tonal noise attenuation, the interest of the present investigation is focused on broadband noise attenuation. The plasma actuators were designed and installed on the surface of the bluff body model. The flow around the model was manipulated by the externally applied body force. Through modifying the wake flow behind the model, the flow induced noise at broadband frequency range was expected to be reduced. The effectiveness of the noise attenuation by the plasma actuators was firstly studied by performing far field acoustic measurements in an anechoic facility. Both sound pressure level (SPL) and overall sound pressure level (OASPL) were examined. To provide insight into the noise control mechanism from aerodynamic side, the natural and forced flow fields were subsequently measured and visualised by particle imaging velocimetry (PIV) in a low speed wind tunnel. The next two sections describe the experiments and discuss results. A summary of the present work is provided at the end of the paper.

*Lecturer, Aeronautics and Astronautics, School of Engineering Sciences. AIAA Member.

†Professor, Aeronautics and Astronautics, School of Engineering Sciences. Associated Fellow AIAA.

‡Professor, Aeronautics and Astronautics, School of Engineering Sciences.. AIAA Member.

II. Experimental Methods

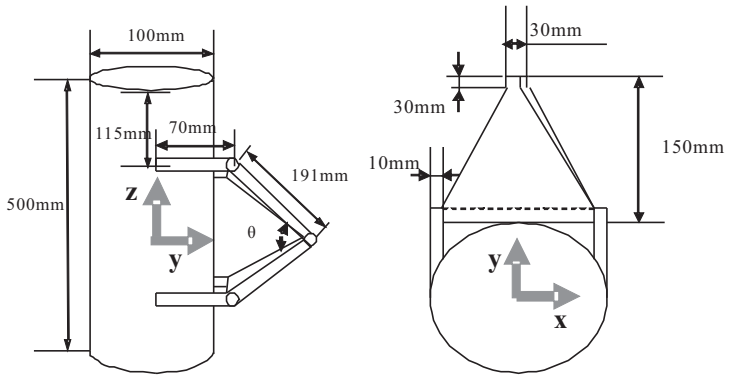

Figure 1. Schematic of the model.

The bluff body tested in this work is a simplified model of bogie beam parts installed on a landing gear, including a cylinder and a strut. The former one corresponds to the main leg of the landing gear, and the latter one corresponds to the torque link of the landing gear. The diameter of the cylinder is 100 mm. The height of the cylinder is 500 mm. The angle θ of the torque link is 45 deg. Additional geometry information of the model, along with the coordinates employed in the PIV measurements, are given in Figure 1. The origin of the coordinates is on the center point of the cylinder.

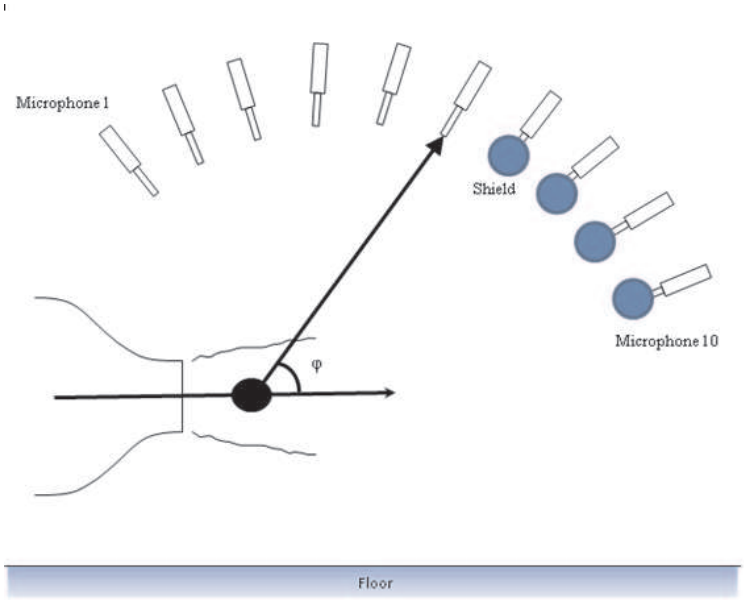

Figure 2. Far field acoustic measurement in an anechoic facility.

The model was tested in an anechoic chamber to examine its far field acoustic properties. Figure 2 shows the testing units in the anechoic chamber. There are 10 microphones installed on an arc that is approximately 2 m away from the model. The elevation angle ϕ of each microphone is 115, 105, 95, 88, 78, 68, 55, 48, 38, 30 deg, respectively. The last four microphones were covered by shields to alleviate the wake effect on acoustic measurement. For each microphone the lowest sensitive frequency is 20 Hz and the highest one is 20 kHz; the sensitivity is -44 ± 5 dB (0 dB$= 1$ V/pa at 1 kHz); the signal-to-noise ratio is more than 58 dB. The microphones' output was passed through preamplifiers and anti-aliasing filters and subsequently was sampled with a data acquisition system produced by National Instruments at 44.1 kHz. A 4096 point fast Fourier transform with a Hanning window function was applied to the sampled data. The spectral results were averaged over 50 signal blocks for statistical confidence.

A nozzle connecting to the plenum chamber can produce a jet flow with the speed up to 30 m/s in the experiments. Reynolds number is up to 2.1×10^5 based on the cylinder diameter. The bluff body model was installed 300 mm down-

stream of the nozzle exit. The power supply of the plasma actuators was located in a separate room to prevent its cooling fan noise from polluting the sound measurements in the anechoic chamber facility. The AC voltage at O(kV) was applied to the plasma actuators via a 20 m length high voltage cable, whose impedance is unknown. As a result, the impedance matching network of the power supply worked inefficiently. For the present configuration the plasma actuators performed efficiently at 6 to 7 kHz with the most uniform and the brightest plasma, which normally corresponds to the maximal body force. To use the plasma actuator at higher frequency beyond 20 kHz, which is outside of the frequency range of human hearing, a new impedance matching network should be designed according to the impedance values of the power supply, cables and the plasma actuators. This can be solved as soon as the plasma actuator design scheme is finalized.

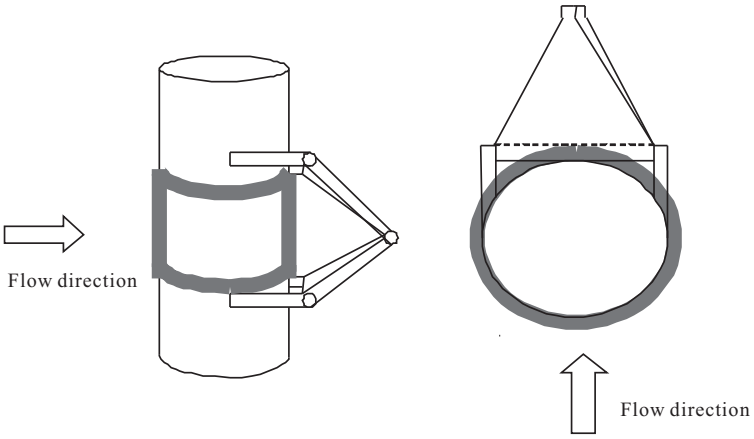

Figure 3. Side view and ceiling view of a passive flow control on the model.

Figure 3 shows a passive flow control method that was implemented by covering the cylinder surface with rubber material, whose thickness is 5 mm that reduces the interaction between the strut and the cylinder wake. Compared to the baseline case without the rubber, the width of the wake is increased that subsequently leads to reduced flow strength impinging on the strut. As a result, the sound generated in the wake-strut interaction is attenuated. Figure 4 shows far field SPL results obtained by a single microphone in the anechoic chamber facility. It can be seen that the SPL at the broadband frequency range (from 1 to 10 kHz) were reduced by up to 10 dB. The noise reduction, however, is small when the rubber thickness is less than 3 mm.

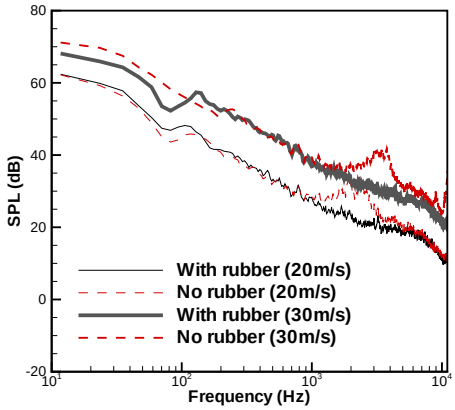

Figure 4. Sound level reduction by the passive flow control method.

Although the passive control method works effectively, the attention is focused on active control methods with the plasma actuators to avoid the need to change the aerodynamic surface extensively. The plasma actuators were designed and produced by flexible printed circuit board (PCB) technology to cover the whole cylinder surface. Kapton is the general dielectric material used in commercial flexible PCB production. The thickness of the Kapton material is 0.5 mm that is selected for its flexibility and for preventing electric breakdown. In the experiments the AC power supply with up to 20 kV peak-to-peak voltage (V_{pp}) was applied to the plasma actuators. More details of the AC power supply and the

plasma actuators can be found in literatures.[3–6]

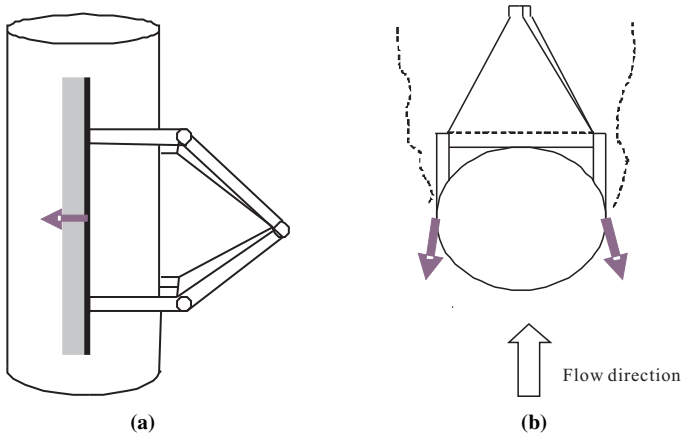

Figure 5. Schematic of the plasma actuator installed on the model.

Figure 5 shows the plasma actuator installed on the model. The plasma actuator consists of two pairs of electrodes, which are installed at $\Omega = 0$ and 180 deg (ω is showed in Figure 1). Other configurations were also extensively tested. It was found that the installation angles slightly below 0 and above 180 deg were also good. However, the installation angles between 0 and 180 deg were found to be less efficient for wake flow control. In Figure 5 the black line denotes the top electrodes exposed to air. The gray lines denote the bottom electrodes that are insulated from the top electrodes and the aluminium model surface by two layers of Kapton material, which is not shown in Figure 5 for simplicity. The overall thickness of the plasma actuator is 1 mm. The arrows in Figure 5 indicate the body force direction that is tangential to the model surface. Under the current configuration with the upstream actuation, the separation from the cylinder was expected to be enhanced, leading to reduced wake-strut interaction. On the other hand, downstream actuation can reduce the width of the wake from a single cylinder[10] and suppress the vortex shedding. The downstream actuation was therefore presumed to increase wake impinging on the strut and thus not a preferable solution for the present investigation.

To study the flow changes due to plasma actuation, PIV measurements were conducted in a low speed wind tunnel facility at the University of Southampton. The wind tunnel is of a closed jet, open loop design. The maximum flow speed attainable in the working section of the tunnel is 30 m/s. The working section has a uniform cross section that measures 0.9 m wide $\times 0.6$ m high. The PIV system used in the experiments is a product of Dantec Measurement Systems and incorporates two Gemini Nd:YAG lasers by New Wave Research that are capable of running at 4 Hz emitting 120 microjoule pulses at 532 nm. A Dantec HiSense (type 13 gain 4) 1024×1289 resolution charged coupled device camera was used to capture flow field of $x - y$ plane at different z value, in double frame mode for image capture. The lenses available were a Nikon Nikkor 24 mm f/2.8 lens and a Nikon Nikkor 60 mm f/2.8 lens. To provide seeding for the flow a Safex S195G smoke seeder using Regular DJ Mix Fluid by Marin Professional was used. The typical size of the non-spherical particles is $2\,\mu$m in diameter. The particles provided suitable tracer material that was homogeneously distributed into the flow. The seeder was placed in the same room as the wind tunnel and care was taken so that the presence of the seeder would not interfere with the flow around the wind tunnel. Image correlations were performed using Dantec's FlowManager to obtain velocity vectors. Typically image sets were processed using an adaptive correlation with a minimum pixel sized interrogation area of 16×16 with a $75\% \times 75\%$ overlap to improve the resolution of the vector map. The processing technique produces a vector map containing up to 317×253 vectors. Inevitably spurious vectors arise as a result of the finite number of tracer particles in the flow, excessive particle displacements, insufficient resolution or even poor image quality. The method for removing these spurious vectors is by using a range validation whereby vectors that are greater than a specified magnitude would be rejected. To produce the time-mean flow, 200 instantaneous vector maps were generated from images collected with 2 Hz sampling rate.

III. Results

To quantitatively compare the noise control performance, SPL results obtained in the anechoic chamber tests were examined. A fixed testing procedure was followed. Firstly, the actuators were installed on the intended test position; secondly, the acoustic data were collected without plasma actuation; finally, the acoustic data were acquired with plasma actuation. The procedure was repeated at different flow speeds and voltages (V_{pp}). Normally, higher voltage led to better

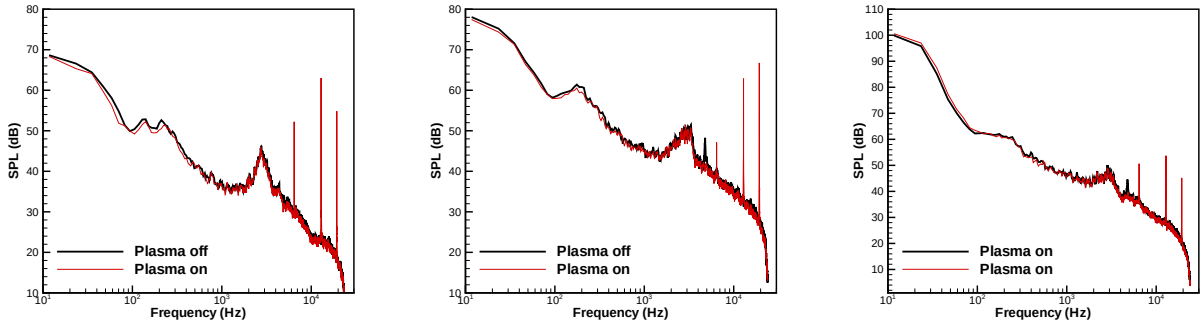

(a) (b) (c)

Figure 6. SPL results of microphone 2, 6, and 9.

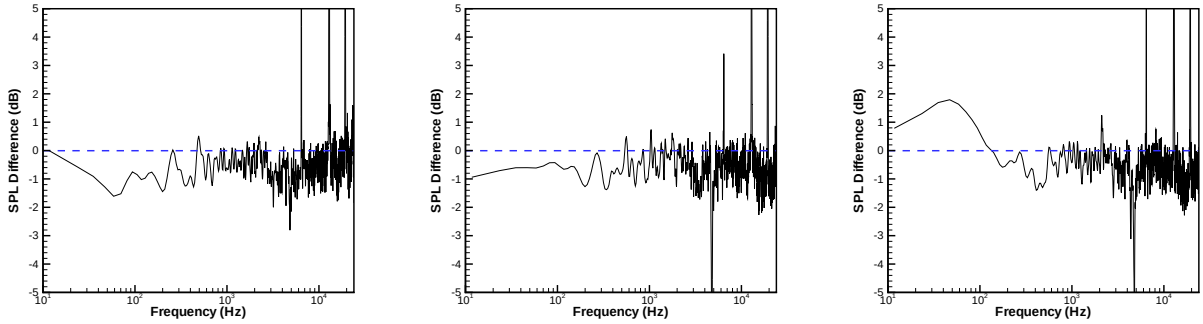

(a) (b) (c)

Figure 7. SPL differences of microphones 2, 6, and 9, where the SPL difference is the SPL value with upstream plasma actuation minus the SPL value without plasma actuation.

control performance. However, the plasma actuators could be broken down by V_{pp} above 20 kV.

Figure 6 shows SPL results of three microphones at $U_\infty = 30$ m/s and $V_{pp} = 15$ kV. To illustrate the noise control performance clearly, the difference between the SPL values with/without plasma actuation is given in Figure 7, where the negative value denotes noise reduction due to plasma actuation, and vice versa. It can be seen that with the upstream actuation, there are broadband noise reduction recorded at microphones 2 and 6. Similar discovery was found in SPL recorded at microphones 1 to 7. However, there is up to 2 dB increase in the low frequency range recorded at microphone 9, which is almost in the wake flow. Microphone 10 is also immersed in the wake flow and produces the similar results. The results from microphone 9 and 10 suggest that, due to the upstream actuation, the wake is more turbulent that produces more noise in low frequency range. On the other hand, the results from microphone 1 to 7 imply that there is a broadband noise reduction outside the wake flow area. It is also worth noting that better noise reduction performance was obtained at a lower speed of $U_\infty = 20$ m/s. In addition to the broadband noise reduction, the plasma actuator also radiates tonal noise at its driving frequency and harmonics. The undesirable sound effect can be removed by increasing the driving frequency beyond 20 kHz with modified impedance matching network, which should be designed as soon as the specifications of the plasma actuator, power supply and cables are finalized for the desired application.

1/3 octave band spectrum results for the data recorded at microphones 2, 6, and 9 are showed in Figure 8. The frequency band is from 125 to 5000 Hz, set below the plasma driving frequency (6.5 kHz) to avoid its negative impact on the 1/3 octave band averaged results. To show the control effect clearly, the difference of 1/3 octave band spectrum with/without the plasma actuation is showed in Figure 9. It can be seen that noise attenuation is up to 1.5 dB, and is most effective in the frequency ranges below 100 Hz and above 2500 Hz for microphone 1 to 7. The noise attenuation effect in the low frequency range for microphones 9 and 10, however, is reduced.

During the test, although all circuits were shielded to prevent electromagnetic interference from plasma discharges,

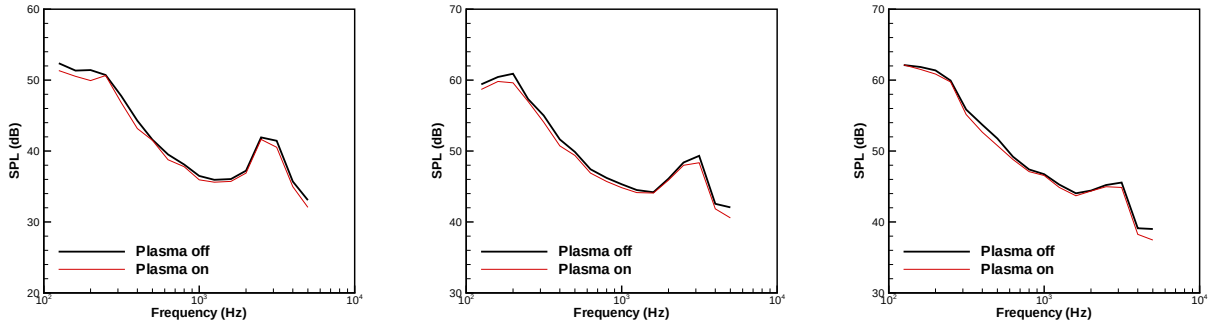

(a) (b) (c)

Figure 8. 1/3 octave band spectra results of microphones 2, 6, and 9.

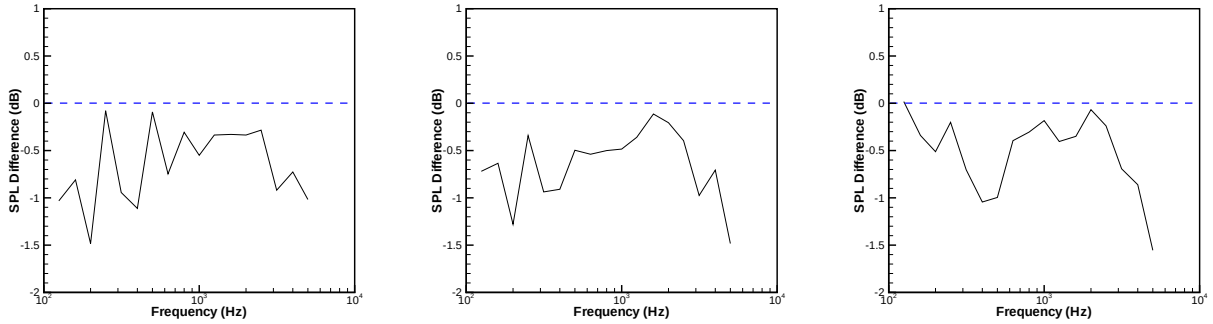

(a) (b) (c)

Figure 9. 1/3 octave band spectra differences of microphone 2, 6, and 9.

the data recorded at microphone 8 was still corrupted and is not used here. In addition, the last microphone in the arc (microphone 10) was immersed in the wake and produced much higher SPL in low frequency range under the plasma actuation, leading to the OASPL increase rather than a reduction. Here only results recorded at microphones 1 to 7 and microphone 9 under upstream plasma actuation are showed in polar coordinates in Figure 10, where the OASPL reduction values are indicated on the radius axis, and the elevation angle of each microphone is on the angle axis. To avoid the inclusion of the plasma radiation noise in the OASPL computation, the frequency range from 125 to 5000 Hz was considered again. It can be seen that, except at microphone 9, the OASPL reductions at all other microphones are about 1 dB.

The sound reduction with the upstream actuation was presumably caused by reducing the wake impinging on the strut. To provide further insight into physics, the time-mean flow results obtained by the PIV measurements were examined. Figure 11 compares the mean velocity U in the x direction with/without the plasma actuation. Two different lines in the observed plane are compared. The first line is normal to the joint that connects the cylinder and the strut. The second line is normal to the strut. The specific coordinates of the two lines are: $y = 16\,\text{mm}$, $z = 135\,\text{mm}$; and $y = 120\,\text{mm}$, $z = 80\,\text{mm}$. Figure 11 shows that U velocity with the plasma actuation is larger than U velocity without the plasma actuation, implying that the wake impinging on the strut could be reduced under the upstream plasma actuation. The PIV measurements were on the joint of the strut at $y = 180\,\text{mm}$ and $z = 0\,\text{mm}$, where little difference in U was found. It implies that the plasma actuation just works effectively on flow field local to the plasma actuators.

Two-dimensional mean flow field results on the $x - y$ plane at $z = 80\,\text{mm}$ are showed in Figure 12. A white coloured block in Figure 12(b) excludes an imperfection area of the sampled flow. The dashed lines in Figure 12(a) and Figure 12(c) denote the laser sheet positions on the strut, on which the wake is supposed to impinge. Compared to Figure 12(a), Figure 12(c) shows that the impinging was reduced with the upstream plasma actuation. On the other hand, Figure 12(b) and Figure 12(d) show that V velocity in the y direction was affected little by the upstream actuation.

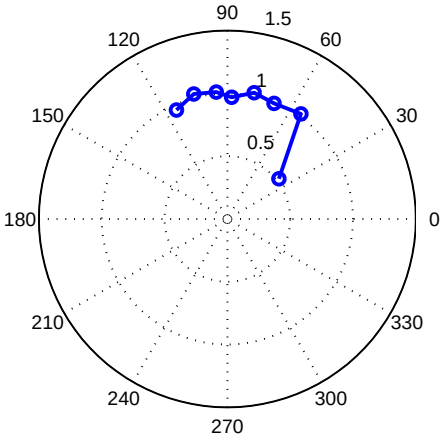

Figure 10. OASPL reduction due to the plasma actuation.

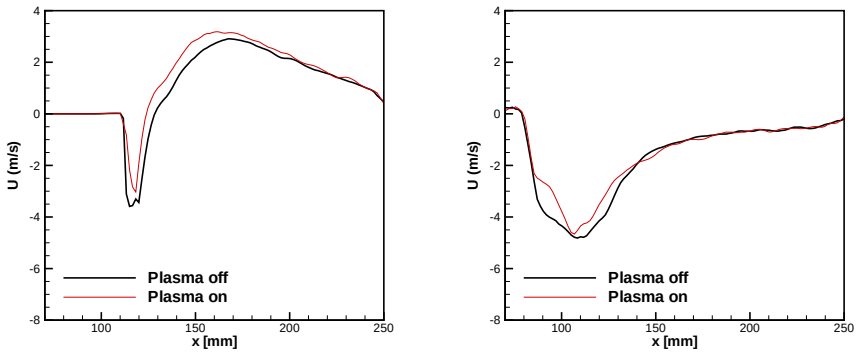

(a) **(b)**

Figure 11. The velocity U in the x direction at: (a) $y = 16$ mm, $z = 135$ mm; and (b) $y = 120$ mm, $z = 80$ mm.

The preliminary results suggest that the flow separation on the bluff body is enhanced by using upstream plasma actuation. It was found that the flow separation enhancement was reduced along with the increase of the free-stream speed. For example, the changes in the aerodynamic field at 30 m/s were not so distinctive as the changes at 20 m/s. Compared to the noise control results by the passive control method (Figure 4), the active control results reflect the fact of the limited authority of the current plasma actuators, which generate an ionic wind of approximately 4 m/s at 1 mm above the dielectric surface according to the previous measurements. In this work the Kapton material was selected for the easy production of the plasma actuators by employing commercial flexible PCB technique. It was found that the induced ionic wind speed can be up to about 8 m/s if the Kapton dielectric material was replaced with 1 mm thickness silicon rubber, where, however, the electrodes of the plasma actuator have to be positioned manually. To better attenuate noise from the bluff body, new actuators based upon silicon rubber will be produced and tested next.

IV. Summary

The aim of this experimental investigation was to investigate the broadband noise attenuation potential of upstream plasma actuation on a bluff body. The plasma actuators were applied to the bluff body surface at free-stream speed up to $U_\infty = 30$ m/s. Both far field microphone measurements in an anechoic chamber facility and PIV surveys of turbulent

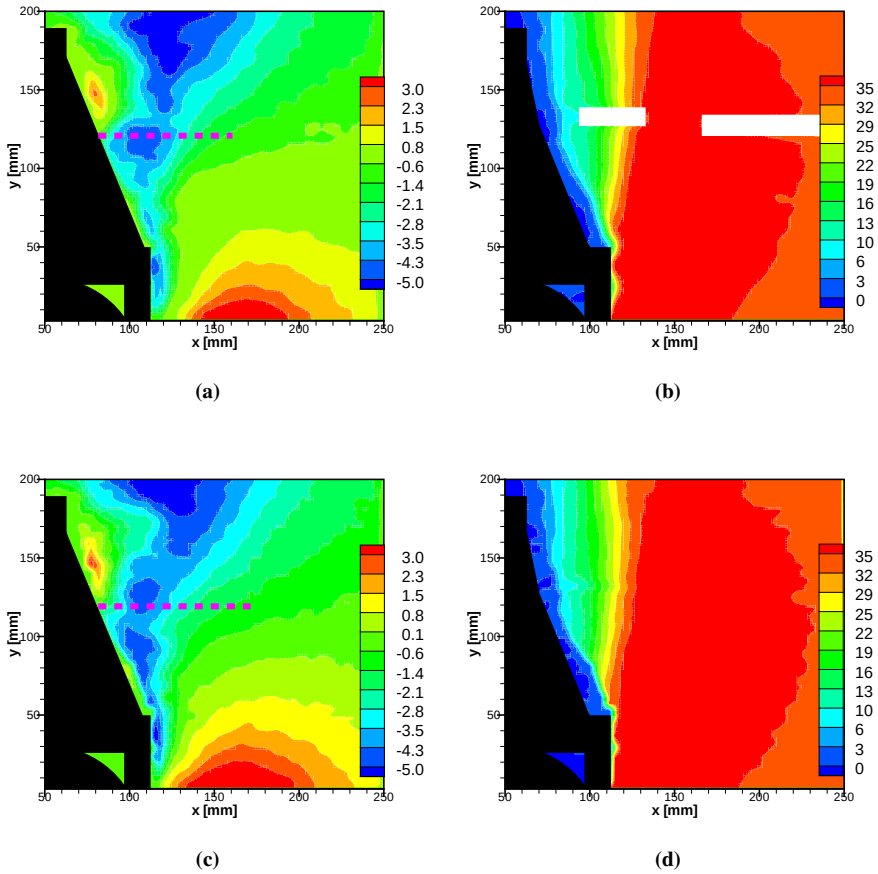

Figure 12. The velocity field, where (a)-(b): without plasma actuation, (c)-(d): with upstream actuation, (a),(c) is U in the x direction, and (b), (d) is V in the y direction.

wake flow in a low speed wind tunnel facility were performed. The microphone measurements show that the far field OASPL values at broadband frequency range can be reduced by about 1 dB with the upstream plasma actuation. Rather than suppressing vortex shedding that generates the tonal noise components in the noise spectrum, the broadband noise reduction is achieved by affecting the interaction between the cylinder wake and the strut. This observation is supported by flow field measurements using PIV. The flow field results local to the junction of the cylinder and the strut, and on the strut were examined by PIV. It can be seen that the speed of the wake impinging on those places is reduced. The same finding was also recorded at other places local to the strut. To further reduce noise, additional wake-strut interaction attenuation should be achieved by increasing the plasma actuator performance. The work is ongoing and beyond the scope of this paper.

Compared with other alternatives, the plasma actuators have many merits, including: simple and cheap implementation of the plasma actuator, direct installation of the plasma actuators on aircraft structure surface and thus impose small effect on overall structure, and rapid time response.

Acknowledgments

This work was supported by TIMPAN (Technologies to IMProve Airframe Noise) project, which is co-funded by the European Commission within the sixth Framework Programme (2002-2006). We would like to acknowledge Stephen Chow of Airbus for helpful discussions.

References

[1]Raman, G. and McLaughlin, D. K., "Recent aeroacoustics research in the United States," *Noise & Vibration Worldwide*, Vol. 31, No. 10, 2000, pp. 15–20.

[2]for Aeronautics Research in Europe, A. C., "Strategic Research Agenda," Vol. 1 and 2, 2002.

[3]Chan, S., Zhang, X., and Gabriel, S., "The attenuation of cavity tones using plasma actuators," *AIAA Journal*, Vol. 45, No. 7, 2007, pp. 1525–1538.

[4]Huang, X., Chan, S., and Zhang, X., "An atmospheric plasma actuator for aeroacoustic applications," *IEEE Transactions on Plasma Science*, Vol. 35, No. 3, 2007, pp. 693–695.

[5]Huang, X., Chan, S., Zhang, X., and Gabriel, S., "Variable structure model for flow-induced tonal noise control with plasma actuators," *AIAA Journal*, Vol. 46, No. 1, 2008, pp. 241–250.

[6]Huang, X. and Zhang, X., "Streamwise and Spanwise Plasma Actuators for Flow-Induced Cavity Noise Control," *Physics of Fluids*, Vol. 20, No. 3, 2008, pp. 037101–1–037101–10.

[7]Roth, J. R., "Aerodynamic flow acceleration using paraelectric and peristaltic electrohydrodynamic effects of a one atmosphere uniform glow discharge plasma (OAUGDP)," *Physics of Plasmas*, Vol. 10, No. 5, 2003, pp. 1166–1172.

[8]Roth, J. R., "Electrohydrodynamically induced airflow in a one atmosphere uniform glow discharge surface plasma," *IEEE International Conference on Plasma Science*, , No. 6P-67, June 1998.

[9]Roth, J. R., Sherman, D. M., and Wilkinson, S. P., "Electrohydrodynamic flow control with a glow-discharge surface plasma," *AIAA Journal*, Vol. 38, No. 7, July 2000, pp. 1166–1172.

[10]Thomas, O. F., Kozlov, A., and Corke, C. T., "Plasma Actuators for Landing Gear Noise Reduction," AIAA Paper 2005-3010, 2005.

[11]Sung, Y., Kim, W., Mungal, M. G., and Cappelli, M. A., "Aerodynamic modification of flow over bluff objects by plasma actuation," *Experiments in Fluids*, Vol. 41, 2006, pp. 479–486.

[12]Moreau, E., "Airflow control by non-thermal plasma actuators," *J. Phys. D: Appl. Phys.*, Vol. 40, 2007, pp. 605–636.

[13]Forte, M., Jolibois, J., Pons, J., Moreau, E., Touchard, G., and Cazalens, M., "Optimization of a dielectric barrier discharge actuator by stationary and non-stationary measurements of the induced flow velocity: application to airflow control," *Experiments in Fluids*, Vol. 43, No. 6, 2007, pp. 917–928.